Lecture 13: Molecular Devices

Last time:	biological strategies for inorganic templating by organic materials Biomimetic organic template materials Biomimesis of bone
Today:	molecular devices
Reading:	V. Vogel, 'Reverse engineering: Learning from proteins how to enhance the performance of synthetic nanosystems,' *MRS Bull*. **Dec**. 972-978 (2002)

Overview to date

Current Road Map of the course:

- Started with degradable synthetic polymers – structural and controlled release materials
- Discussed modifying degradable materials for biological recognition
- Moved to controlled release devices fabricated from degradable polymers
- Next, hydrogel materials for drug delivery, tissue engineering, and lab-on-a-chip applications
  - Structure, what are they made of
  - Theory of gel swelling for neutral and ionic gels
- Biomineralization: approaches used by biology and how we are trying to mimic them
  - Future materials for hard tissue engineering

- So far, largely looking at 'macroscopic' materials
  - Materials from which micron-sized or larger scaffolds, drug delivery devices and gels are fabricated
- Moving to smaller length scales: molecules and aggregates of molecules, we come to some new applications
  - Performing molecular-level functions
  - Delivering molecular cargos to cells (labeling or treating cells)

Application areas we'll focus on:

- Molecular devices
  - (Length scale of one or a few molecules)
  - Single-molecule switches
  - Molecular motors
- Nano- to micro-scale drug carriers and detection reagents
  - (Length scale of supramolecular aggregates to many-molecule aggregates)
- Drug targeting

Molecular Devices

Current Approaches to Molecular Devices based on Protein-polymer hybrids

- 3 examples we'll discuss:
  1. Use synthetic polymers to control 'on' and 'off state of a protein
  2. Use engineered surfaces to direct the function of proteins
  3. Use engineered proteins to build nano-motorized devices on surfaces

Single-molecule switches

- Using LCST polymers as the basis of a molecular switch[1]
  - LCST polymers show sharp volume change at the transition temperature as they transform from swollen coil to globule

Poly(N-isopropylacrylamide)

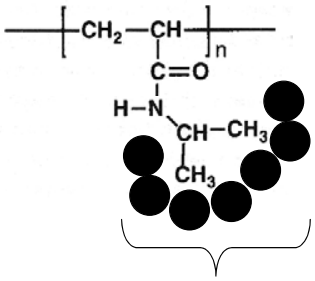

ordered water molecules
(minimize water-hydrophobe contacts)

↓ Dehydration allows water to disorder (*entropically-driven*)

$\Delta S = S_{dehydrated} - S_{hydrated} > 0$

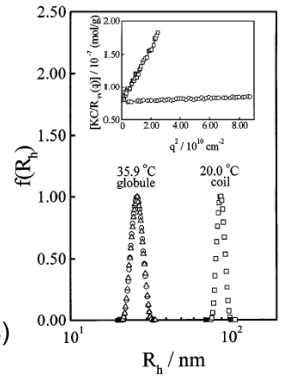

FIG. 1. Typical hydrodynamic radius distribution $f(R_h)$ of poly(*N*-isopropylacrylamide) chains in deionized water at two different temperatures, where polymer concentration is 6.7×10^{-7} g/mL. At 35.9 °C, o represents $f(R_h)$ just after the temperature reached equilibrium; and Δ after ~33 h. The inset shows the angular dependence of the Rayleigh ratio $[R_{vv}(q)]$ of the polymer chains, respectively, in the coil (□) and globule (o) states.

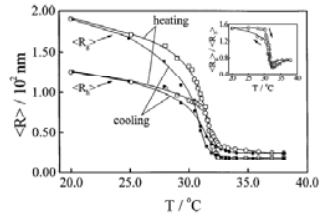

FIG. 2. Temperature dependence of the average radius of gyration $\langle R_g \rangle$ and the average hydrodynamic radius $\langle R_h \rangle$, respectively, in the coil-to-globule (heating) and the globule-to-coil (cooling) processes, where each point was obtained at least 2 h after the solution reached the thermal equilibrium to ensure that the polymer chains were thermodynamically stable. The inset shows the temperature dependence of $\langle R_g \rangle / \langle R_h \rangle$ in the heating and the cooling processes.

(Wu and Wang, 1998)

- ***A temperature-sensitive streptavidin mutant***[2-4]
  - Chime animation of streptavidin with biotin bound to tetrameric pockets: http://www.chem.uwec.edu/Webpapers2001/barkacs/Pages/Steptavidin.html

Poly(N,N-diethylacrylamide):
dehydrates with increasing temperature- analogous to PEG-PPO-PEG triblock copolymers

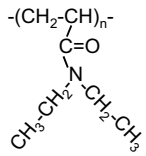

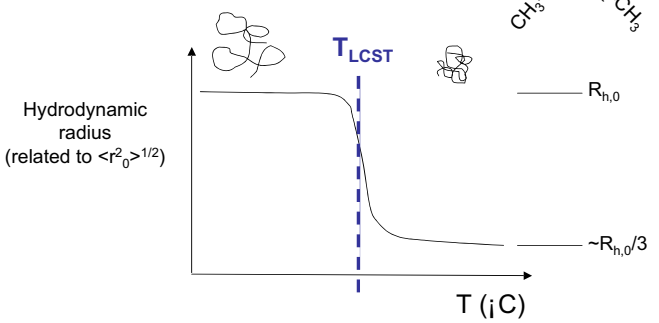

Mutatation introducing cysteine near binding pocket

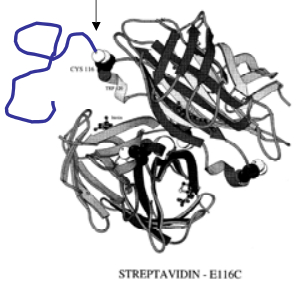

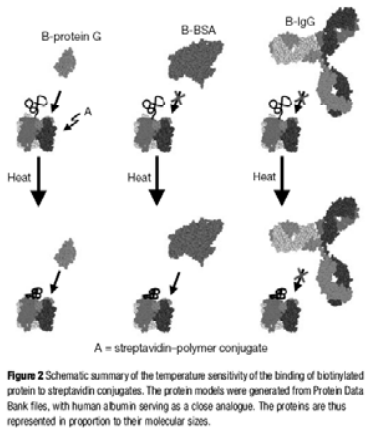

Figure 2 Schematic summary of the temperature sensitivity of the binding of biotinylated protein to streptavidin conjugates. The protein models were generated from Protein Data Bank files, with human albumin serving as a close analogue. The proteins are thus represented in proportion to their molecular sizes.

(Ding et al. 2001)

  - Blockade of access to biotin-binding pocket is dependent on the size of the biotinylated target:
    - Small protein G is not sterically blocked by the hydrated PDEAAm chain
    - Large biotinylated IgG can't access pocket even when PDEAAm chain is collapsed
  - Varying the length of the thermally-responsive chain allows the degree of binding blockade to be tuned (Figure 4)

Polymer switch shows size-selective blockade of streptavidin binding pocket:

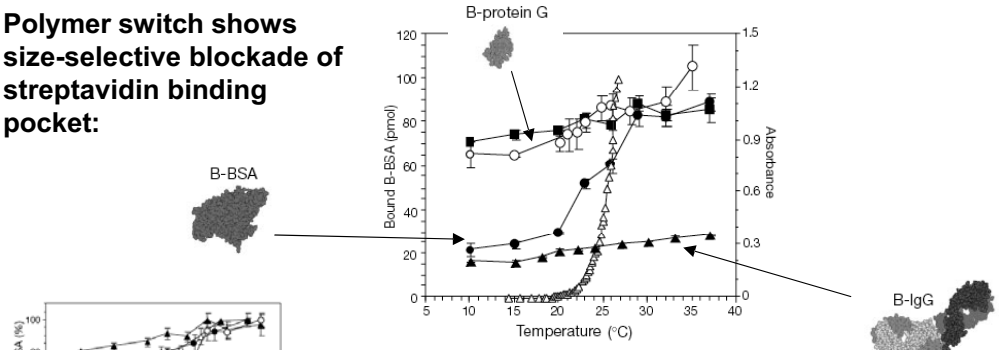

Figure 1 Shielding of biotinylated protein binding to E51K/N118K–PDEAAm conjugates. The binding of biotinylated BSA (B-BSA) to the E51K/N118K–PDEAAm-12.8k conjugate (filled circles) rises significantly as the temperature rises through the LCST (~23 °C), whereas the binding of B-BSA to unconjugated E51K/N118K streptavidin (filled squares) is efficient at all temperatures studied. The much smaller B-protein G binds to the E51K/N118K–PDEAAm-12.8k conjugate (open circles) efficiently over the whole temperature range investigated, while the binding of the large protein B-IgG to the E51K/N118K–PDEAAm-12.8k conjugate (filled triangles) is shielded over the entire temperature range. Under the binding conditions used (see Methods), the E51K/N118K–PDEAAm-12.8k conjugate has an LCST of ~23 °C (open triangles).

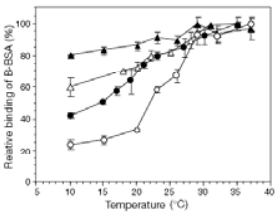

Figure 4 Effect of molecular mass of PDEAAm on the shielding efficiency. The graphs show the binding of B-BSA to E51K/N118K streptavidin (filled triangles) and covalent conjugates of E51K/N118K–PDEAAm with molecular masses of 2.0 kDa (open triangles), 6.7 kDa (filled circles) and 12.8 kDa (open circles). To compare the effect of the different-molecular-mass polymers on the shielding efficiency, we show relative binding of B-BSA, which is obtained by normalizing the amount of bound B-BSA to the maximum binding for each sample.

- Also the basis for triggered *release* switches
  - Expose biotin-loaded conjugates to successive cycles of $T < T_{LCST}$ through $T > T_{LCST}$
    - 4 cycles 'kick out' all bound biotin

All bound biotin released by 4 temperature cycles:

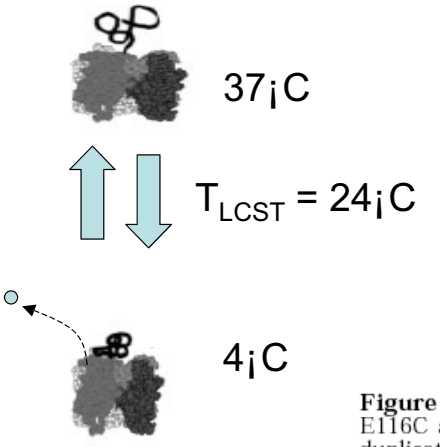

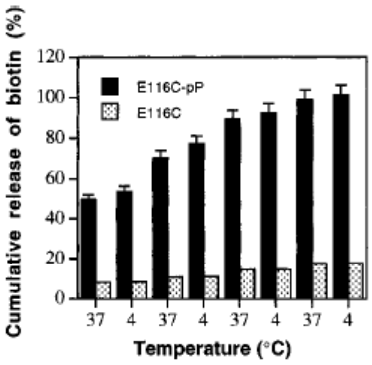

Figure 8. Cumulative release of bound biotin from immobilized E116C and E116C-pP. The data presented are an average of duplicate experiments. Magnetic beads (Dynal M-280) immobilized with 5.4×10^{-10} mol of E116C-pP were used for the assay. Sodium phosphate buffer, pH 7.4, 100 mM was used as the medium.

(Ding et al., 1999)

- Mechanisms for controlling access by large or small ligands
  - Small ligands have access to binding pocket next to immobilized chain blocked when chain is collapsed, but can access the pocket when the chain is hydrated
    - Conversely, if biotin binds in the pocket, collapse of the chain can eject the bound small ligand

- Larger protein ligands are always prevented from accessing the pocket next to the immobilized chain
  - Selective access occurs for the second binding pocket 20 Å away- when the chain is collapsed it does not prevent access to the second pocket, but when hydrated, long chains can prevent access to the neighboring pocket and block protein binding

Mechanisms of switch operation:

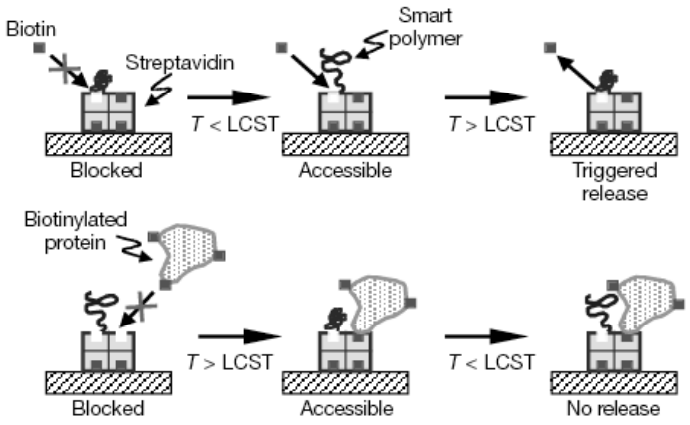

Figure 5 Schematic model of different shielding mechanisms. The model illustrates the shielding effects of a conjugated smart polymer on the binding of a small ligand (biotin) and a large macromolecular ligand (a biotinylated protein) to streptavidin. The polymer is in both cases conjugated to one binding site on the exposed face of an immobilized streptavidin molecule. (Only one polymer chain may be conjugated per binding face, due to steric hindrance). In the case of biotin association, the collapsed polymer blocks biotin access to the same site where the polymer is conjugated, but permits association at that site when the polymer is rehydrated and extended away from the site. In the case of the larger biotinylated protein, the conjugated polymer always blocks binding to the site where the polymer is conjugated, whether the polymer is collapsed or extended. The nearby binding site is exposed and accessible for binding of a biotinylated protein only when the polymer is collapsed, and provided the protein is small enough. Reversal of the stimulus can lead to release (depletion) of the biotin from the binding site where the polymer is conjugated[6,7] but there is no reversal expected for the biotinylated protein because the polymer is conjugated to the subunit 20 Å away from the binding site.

- Fabrication of capture and release devices[3,5]
  - Conjugation to magnetic micro- or nano-spheres
    - Affinity purification

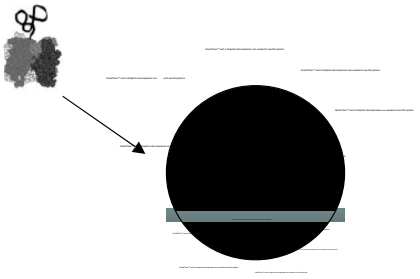

Applications:

- Affinity purification
- Cell-surface labeling
- Responsive drug release

Conjugation to magnetic microspheres/nanospheres

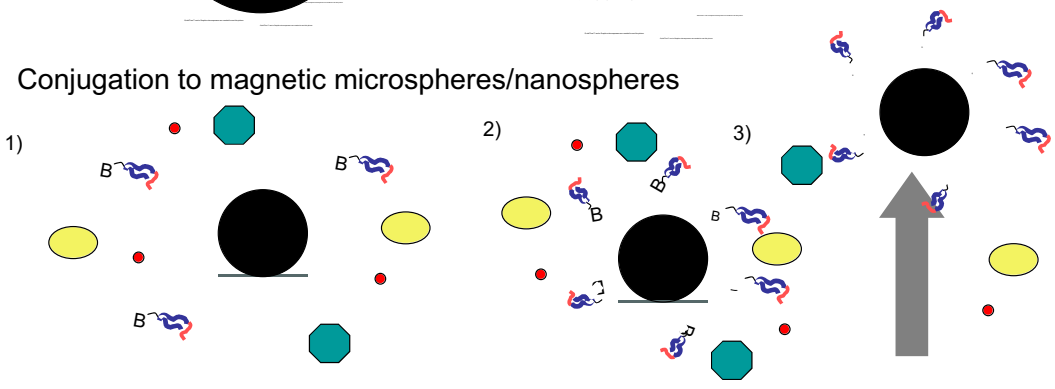

- Generality of concept
  - Switch temperature can be tuned by copolymerizing with more hydrophilic monomers such as hydroxyethyl methacrylate

- Other temperature-responsive polymers that could be used:
  - Poly(N-isopropylacrylamide)
- pH-responsive switches
  - copolymers of PNIPAAm and AAc

Copolymerization allows switch temperature to be varied:

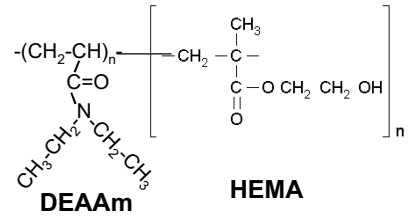

DEAAm **HEMA**

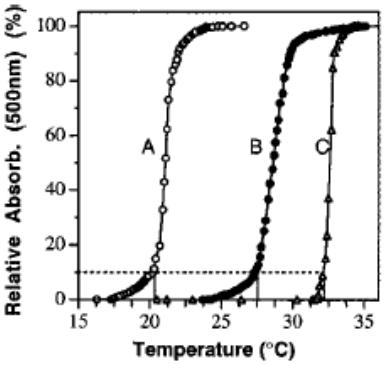

Switches can also be synthesized for light or pH triggering:

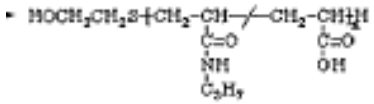

Random Copolymer of NIPAAm-AAc

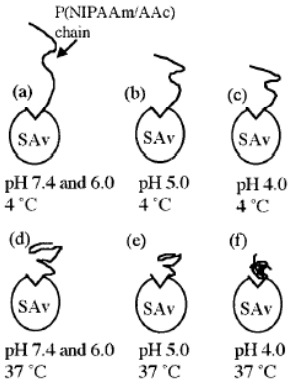

Figure 6. Proposed conformations of the polymer chain coils of poly(NIPAAm-*co*-AAc) conjugated to mutant streptavidin (SAv) at various pHs at 4 and 37 °C.

Molecular Motors[6]

- Engineering principles on which macroscopic engines/motors are based fail at the nano-scale
- How to miniaturize controlled force-generating devices cell-manipulating devices, nanobots, etc.?
  - Molecular motors driven by single-molecule fuels, photons, etc.

Protein motors used by nature for force generation and motion[7]

- Motor proteins convert chemical energy into mechanical force via conformational changes
  - Generation of protein motion along guide-wires: protein filaments
  - Driven by energy released on hydrolysis of adenosine 5'-triphosphate
  - Myosin and kinesin are two examples of ubiquitous motor proteins found in eukaryotic cells
- Kinesin
  - Motor protein translates along 25nm-diameter rigid rods (microtubules, up to 100 μm in length possible in vitro)
  - Transport of molecular cargos through cells
    - Small membrane organelles or protein complexes
    - E.g. encapsulated neurotransmitters from nerve cell nucleus to the synapse to excite neighboring cells
  - Coordination of two heads allows continuous 'walking' along microtubules with 80 Å steps
    - Efficient processive motion allows long-range transport by one or a few motor proteins
    - Motion is directional toward 'plus' end of microtubule
- Myosins
  - Motor protein moves along actin filaments
  - Enables contractile cell functions such as cell motility and muscle contraction
    - Operates in a large array of motors to produce large-scale motions/forces

- ~100 Å per ATP hydrolysis step
- Two heads act independently of one another- single stroke then release from actin polymer
  - Can't continuously march along polymer by itself

Myosin
Muscle motor protein, transport along actin fibers

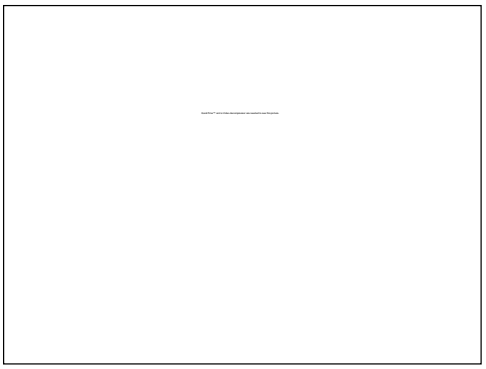

kinesin
transport along microtubules

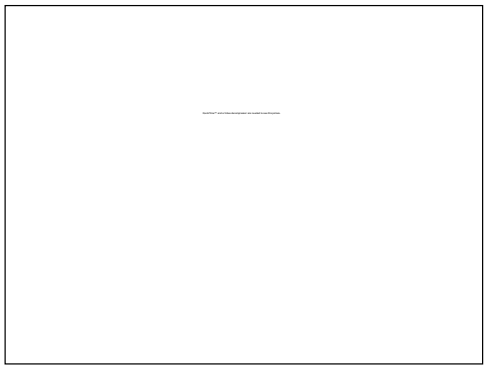

Limitations for use in bioengineering applications:
- unidirectional motion
- Controlling orientation of "cable" and "car"

(Vale and Milligan, 2000)

- Energy source for these molecular motors
  - ATP hydrolysis cycle linked to conformational change cycle
  - Energy gained by binding ATP moves kinesin neck linker from rearward-facing position forward to dock against catalytic core of head
    - Motion of one neck pulls other free from previous microtubule binding site and throws it forward to the next site (~80 Å)
  - Origin or directionality: myosin goes opposite direction from kinesin
    - Directionality comes from conformation matching of head to polymers in one direction combined with time sequence of head release from polymer
    - Both motors have an upstroke on binding ATP, downstroke on hydrolysis
      - Kinesin neck docks onto head on upstroke
      - Myosin: tight binding of head to polymer in ATP-free state
        - Forward motion on upstroke when head releases from polymer
      - Kinesin: tight binding in ATP-bound state
        - Reverse motion on downstroke when head releases from polymer

SHOW SCHEMATICALLY ON BOARD:

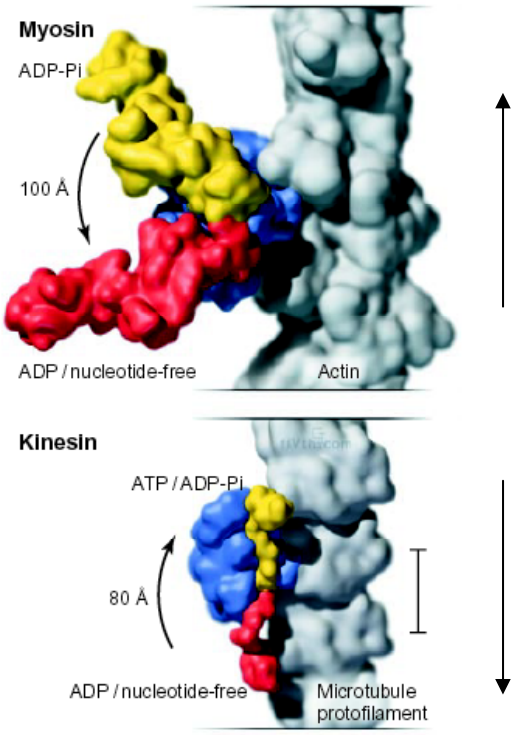

Fig. 4. A model for the "power strokes" of myosin and kinesin motors complexed with their polymer tracks. In myosin, a ~100 Å motion of the lever arm domain is generated when the motor undergoes a transition from an ADP-Pi–bound state to an ADP/nucleotide-free conformation (*78*). This figure was generated by superimposing the structures of smooth muscle myosin (ADP-AlF_4^-) and the nucleotide-free chicken skeletal myosin. Shown are the converter/lever arm positions in ADP-Pi (yellow) and nucleotide-free (red) states, the similar catalytic cores (blue), and the actin filament (gray; "pointed end" toward the top). In the motility cycle of a kinesin dimer (only one head shown here) along a microtubule (a single protofilament is shown in gray; "plus end" toward the top), the neck linker swings from a rearward-pointing position (ADP/nucleotide-free; red) to a forward-pointing position (ATP/ADP-Pi; yellow). The "ATP/ADP-Pi" state is rat conventional kinesin, whereas the "ADP/nucleotide-free" position of the neck linker was modeled on the basis of cryo-electron microscopy from Rice *et al.* (*26*). Myosin and kinesin structures were superimposed using their P-loops, showing that they bind in similar orientations to their tracks. (Note: The actin filament runs parallel to the plane of the image, but the microtubule is tilted ~20° with respect to the plane of the image.) Although the mechanical elements are similarly positioned in kinesin and myosin, the power strokes occur in opposite directions (arrows) because of the different polymer binding cycles of the two motors (see text for details). Scale bar, 80 Å.

Some of Matt Lang's work?

Engineering devices for nanoscale assembly using nature's motors (Hess et al. 2001)

- Question: How can we manipulate, move, and assemble objects with nanoscale sizes? E.g. individual proteins, nanocrystals, etc.
  - AFM probe tip- one by one- too slow to be really useful in biosensors, lab-on-a-chip or other materials applications
  - Alternatives?

- Surfaces with microtubule nano-cargo carriers (Hiratsuka et al.[8])
  - Discovered that kinesin molecules adsorbed to a surface could be used to drive random motion of microtubules in 2D
    - Researchers sought to use photolithographically patterned surfaces to gain control over motion and develop nano-carriers with directed motion

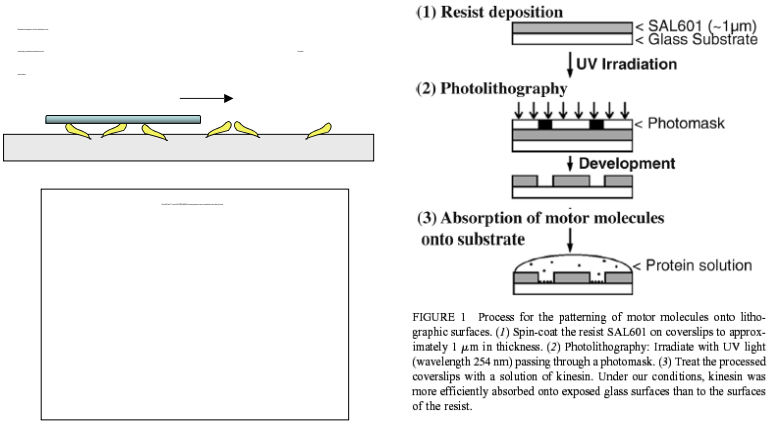

FIGURE 1 Process for the patterning of motor molecules onto lithographic surfaces. (*1*) Spin-coat the resist SAL601 on coverslips to approximately 1 μm in thickness. (*2*) Photolithography: Irradiate with UV light (wavelength 254 nm) passing through a photomask. (*3*) Treat the processed coverslips with a solution of kinesin. Under our conditions, kinesin was more efficiently absorbed onto exposed glass surfaces than to the surfaces of the resist.

(Hiratsuka et al, 2001)

- Simple approach: tracks etched in a photoresist, exposing glass
  - Kinesin motors adsorbed randomly onto exposed glass under conditions where adsorption to resist was minimal (high ionic strength and 0.1% tween surfactant present during adsorption)
  - Circular tracks:
    - Tracks confine motion of microtubules approximately linearly forward or backward
    - No arrowheads: microtubules walk in both directions around circles
    - With arrowheads: microtubules on inside track move counter-clockwise, microtubules on outer track move clockwise
      - Arrowheads act as directional rectifiers, moving against direction of arrow, high probability of microtubule striking wall and reversing direction as it jumps to new set of kinesin molecules
      - Steady motion observed up to 2 hrs in the presence of ATP

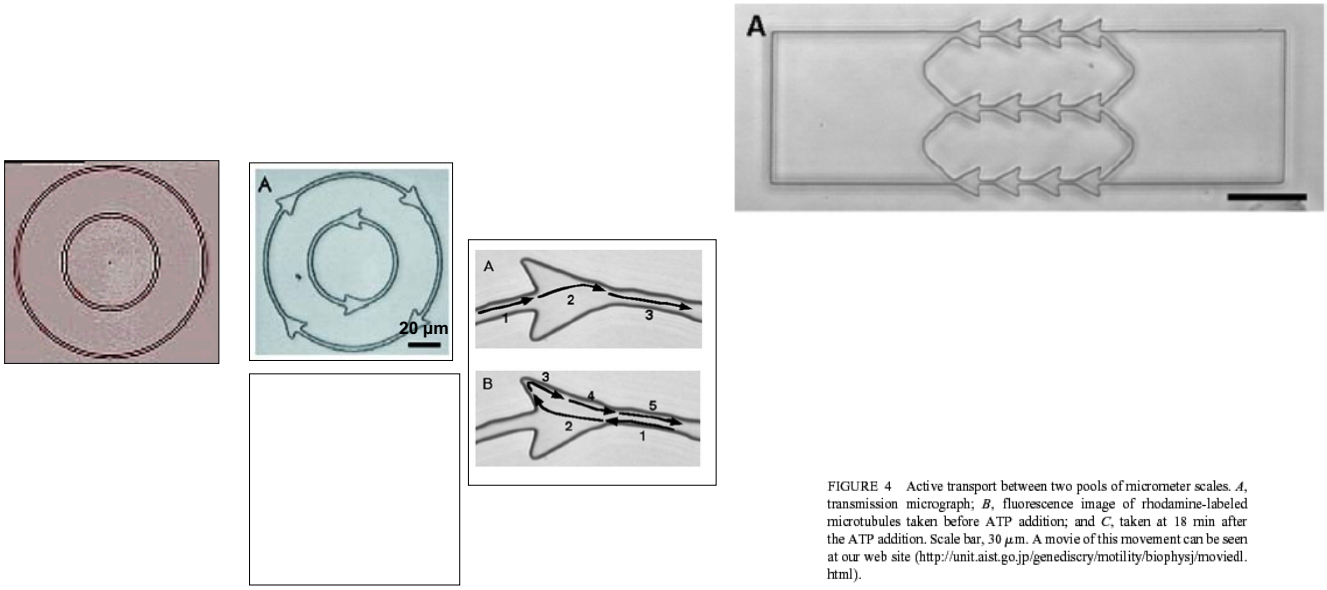

FIGURE 4 Active transport between two pools of micrometer scales. *A*, transmission micrograph; *B*, fluorescence image of rhodamine-labeled microtubules taken before ATP addition; and *C*, taken at 18 min after the ATP addition. Scale bar, 30 μm. A movie of this movement can be seen at our web site (http://unit.aist.go.jp/genediscry/motility/biophysj/moviedl.html).

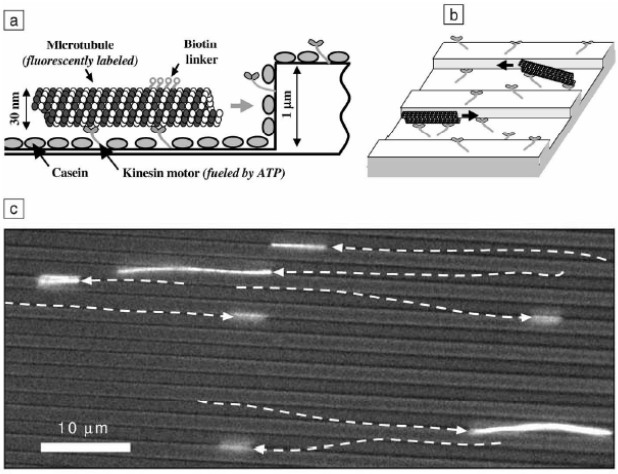

Figure 5. Engineering a cargo-transport system at the nanoscale: a molecular shuttle made from motor proteins moving on engineered tracks. (a) Schematic illustration of the principle. A photolabeled microtubule is propelled in open microfabricated channels [seen as dark stripes in (c)] by surface-bound kinesins (motor proteins). The space between the kinesins is filled with the milk protein casein to prevent nonspecific surface adsorption of the microtubules. The microtubule can be functionalized with molecular linkers (e.g., biotin) to hook up cargo. (b) As a microtubule collides with a steep wall, it bends to align itself parallel to the wall or, alternatively, it loses contact with the surface. (c) Micrograph of photolabeled microtubules moving in channels on polyurethane; channels are 2 μm wide. The dotted lines indicate the paths of individual microtubules.

(Vogel, 2002)

- We don't yet understand the physicochemical principles controlling molecular motor speed, unloading/loading of cargo

A molecular rotor built from ATPase

- Question: how do we create engines to provide piconewton forces for nanodevices?
  - One answer: engineered materials based on protein motor-based engines
- Work of the group of Carlo Montemagno at UCLA (Dept. of Bioengineering)[9-13]
- F_1 fragment of adenosine triphosphate synthase (F_1-ATPase)
  - Role of this protein in cell
  - Rotary motion during ATP hydrolysis as γ subunit transitions between 3 equidistant positions around the ATPase complex
    - No-load rotational velocity of ~17 revolutions per second
  - Generates > 80 pN•nm work
  - Approximately 100% efficient!
  - ~10 nm diameter

F_1 fragment of adenosine triphophate synthase (F_1-ATPase)

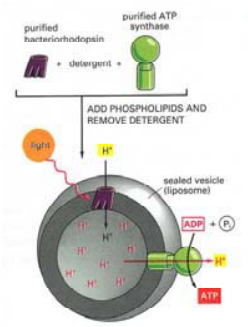

Figure 14–25 ATP synthase. As indicated, the F_1ATPase portion is formed from multiple subunits (*Greek letters*), as is the transmembrane H^+ carrier.

Figure 14–26 An experiment demonstrating that the ATP synthase is driven by proton flow. By combining a light-driven bacterial proton pump (bacteriorhodopsin), an ATP synthase purified from ox heart mitochondria, and phospholipids, vesicles were produced that synthesized ATP in response to light.

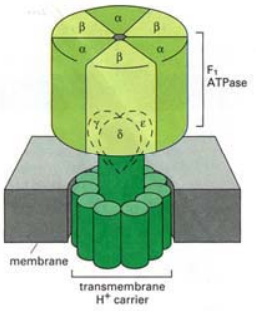

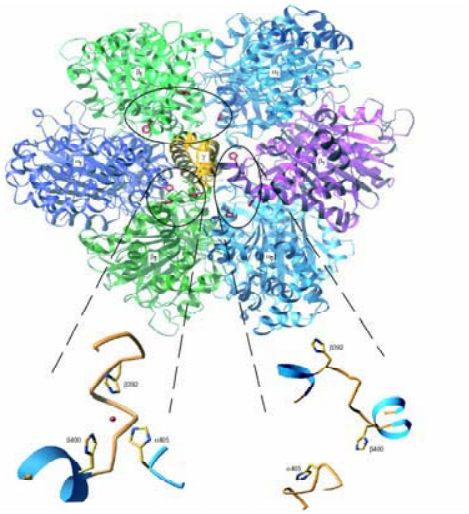

- Montemagno's group prepared mutants of this protein to use as ATP-fueled molecular motors for nanodevices

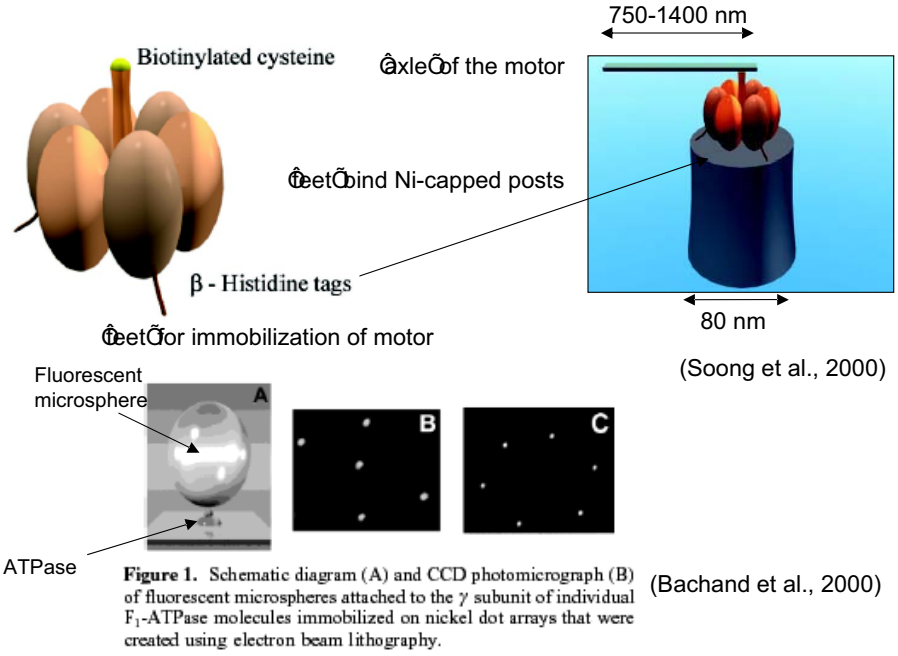

(Soong et al., 2000)

Figure 1. Schematic diagram (A) and CCD photomicrograph (B) of fluorescent microspheres attached to the γ subunit of individual F_1-ATPase molecules immobilized on nickel dot arrays that were created using electron beam lithography.

(Bachand et al., 2000)

ATP-driv

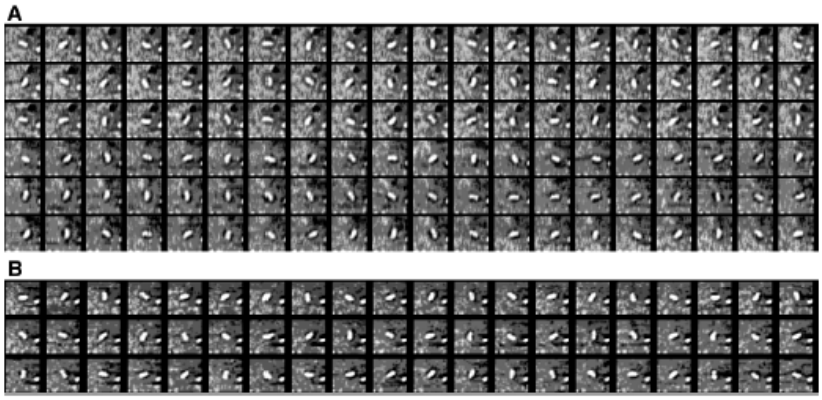

Fig. 2. Image sequence (viewed left to right) of nanopropellers being rotated anticlockwise at 8.3 rps (**A**) and 7.7 rps (**B**) by the F_1-ATPase biomolecular motor. Observations were made using 100× oil immersion or 60× water immersion and were captured with a CCD video camera (frame rate 30 Hz). The rotational velocity ranged from ~0.8 to 8.3 rps, depending on propeller length. Data were recorded for up to 30 min; however, propellers rotated for almost 2.5 hours while ATP was maintained in the flow cell. These sequences can be viewed as movies at the Nanoscale Biological Engineering and Transport Group Web site (http://falcon.aben.cornell.edu/News2.htm).

- Creating motors with a chemical on/off switch[13]
  - Mutated ATP binding face of ATPase to contain a 3-amino acid Zinc ion binding domain (3 histidines)
  - Mutant protein binds zinc and zinc blocks action of motor
    - Classical allosteric enzyme inhibition
  - Chelation of zinc returns motor to active state

Zn^{++} sensitivity of motor:

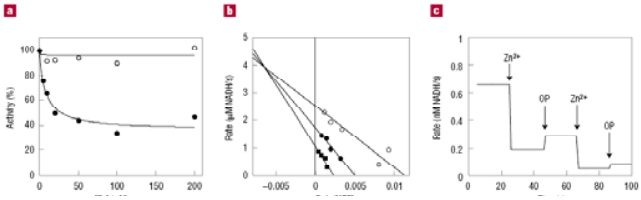

Figure 2 Steady-state kinetics of ATP hydrolysis in the wild-type and mutant TF_1 enzymes. a, The effect of Zn^{2+} addition on the activity of wild-type (DEMH; open circles) and mutant (DEMHZ; filled circles) enzymes. For DEMHZ, Zn^{2+} binding is modelled with a hyperbolic binding isotherm[19], with $^{app}K_d$ = 9.6 μM. **b**, Eadie–Hofstee transformation of the steady-state kinetics of DEMHZ with respect to ATP concentration in the presence of different Zn^{2+} concentrations (open circles, 0 μM; filled circles, 5 μM; squares, 200 μM). **c**, Two cycles of successive additions of 100 μM Zn^{2+} and 150 μM 1,10-phenanthroline (OP).

Turning nanorotors on and off by addition of Zn^{++} and a Zn^{++} chelator:

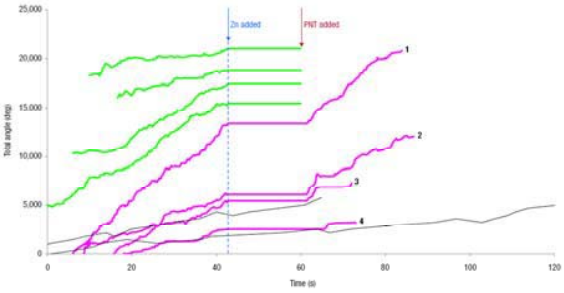

Figure 3 Measurements of single-molecule rotation and control. The movements of rotating fluorescent actin filaments were recorded and digitized. The rotation angle as a function of time is shown for eight filaments attached to the mutant ATPase and two filaments attached to motors without the zinc mutation (black lines). The filaments rotated continuously in the presence of ATP. After the addition of 800 μM $ZnSO_4$ (blue arrow), the filaments attached to the mutant motor stopped, whereas the filaments attached to the wild-type motor continued rotating at the same rate. We added 1,10-phenanthroline (800 μM) to the stopped filaments (red arrow), restarting the motor motion. There was an interval of about 3 s after the addition of both the Zn^{2+} and the phenanthroline in which the filaments were out of focus because the stage position had been disturbed, preventing a more precise determination of the times of stopping and restarting motion. Some filaments were dislodged from the surface during the fluid replacement and so rotation data following the PNT addition are not available (green lines). The data for all filaments have been shifted in time to synchronize the Zn^{2+} addition times. The Zn^{2+} seems to have no lasting effects on the motors. The rotational rates before Zn^{2+} addition and after Zn^{2+} removal are similar, as linear fits of each of the pink traces show: (1) before Zn^{2+} 0.96 rotations s^{-1}, after Zn^{2+} 0.97 rotations s^{-1}; (2) 0.61, 0.61; (3) 0.36, 0.32; (4) 0.27, 0.19. The differences between the numbers in each case are within the variations of rotational rate before Zn addition. The lengths of filaments 1–4 are 1.75 μm, 2.0 μm, 2.25 μm and 2.25 μm, respectively.

- Assembling these hybrid proteins into molecular devices

- Key need for device design: controlled placement of motors on surfaces

Combining the hybrid molecular motor with engineered materials as a step toward nanodevices

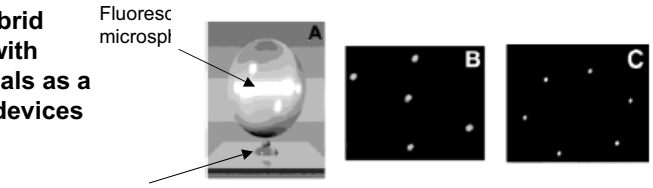

Figure 1. Schematic diagram (A) and CCD photomicrograph (B) of fluorescent microspheres attached to the γ subunit of individual F_1-ATPase molecules immobilized on nickel dot arrays that were created using electron beam lithography.

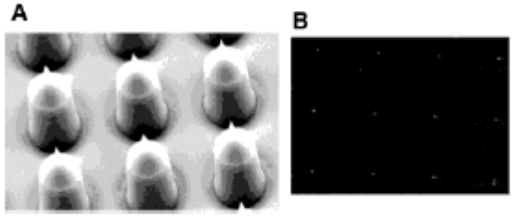

Figure 3. Optical lithography was used to create the nanoimprinting mold (A), which subsequently was used to create large arrays of nickel dots (B). Dots were 50−250 nm diameter and 5−15 nm high.

(Bachand et al., 2000)

References

1. Wu, C. & Wang, X. H. Globule-to-coil transition of a single homopolymer chain in solution. *Physical Review Letters* **80**, 4092-4094 (1998).
2. Ding, Z., Fong, R. B., Long, C. J., Stayton, P. S. & Hoffman, A. S. Size-dependent control of the binding of biotinylated proteins to streptavidin using a polymer shield. *Nature* **411**, 59-62 (2001).
3. Bulmus, V., Ding, Z., Long, C. J., Stayton, P. S. & Hoffman, A. S. Site-specific polymer-streptavidin bioconjugate for pH-controlled binding and triggered release of biotin. *Bioconjug Chem* **11**, 78-83 (2000).
4. Shimoboji, T., Ding, Z., Stayton, P. S. & Hoffman, A. S. Mechanistic investigation of smart polymer-protein conjugates. *Bioconjug Chem* **12**, 314-9 (2001).
5. Ding, Z. et al. Temperature control of biotin binding and release with A streptavidin-poly(N-isopropylacrylamide) site-specific conjugate. *Bioconjug Chem* **10**, 395-400 (1999).
6. Vogel, V. Reverse engineering: Learning from proteins how to enhance the performance of synthetic nanosystems. *Mrs Bulletin* **27**, 972-978 (2002).
7. Vale, R. D. & Milligan, R. A. The way things move: looking under the hood of molecular motor proteins. *Science* **288**, 88-95 (2000).
8. Hiratsuka, Y., Tada, T., Oiwa, K., Kanayama, T. & Uyeda, T. Q. Controlling the direction of kinesin-driven microtubule movements along microlithographic tracks. *Biophys J* **81**, 1555-61 (2001).
9. Montemagno, C. Biomolecular motors: Engines for nanofabricated systems. *Abstracts of Papers of the American Chemical Society* **221**, U561-U561 (2001).
10. Montemagno, C. & Bachand, G. Constructing nanomechanical devices powered by biomolecular motors. *Nanotechnology* **10**, 225-231 (1999).
11. Bachand, G. D. et al. Precision attachment of individual F-1-ATPase biomolecular motors on nanofabricated substrates. *Nano Letters* **1**, 42-44 (2001).
12. Soong, R. K. et al. Powering an inorganic nanodevice with a biomolecular motor. *Science* **290**, 1555-1558 (2000).
13. Liu, H. Q. et al. Control of a biomolecular motor-powered nanodevice with an engineered chemical switch. *Nature Materials* **1**, 173-177 (2002).